A flame propagation model for nanopowders

Audrey Santandrea, David Torrado, Matteo Pietraccini, Alexis Vignes, Laurent Perrin, Olivier Dufaud

A flame propagation model for nanopowders

Audrey Santandrea [a,b], David Torrado [a], Matteo Pietraccini [a], Alexis Vignes [b], Laurent Perrin [a] & Olivier Dufaud [a]

[a] Laboratoire Réactions et Génie des Procédés, Université de Lorraine, CNRS, LRGP, Nancy, France
[b] INERIS, Accidental Risks Division, Parc Technologique ALATA, Verneuil-en-Halatte, France

E-mail: olivier.dufaud@univ-lorraine.fr

Abstract

The determination of explosion severity should be made from intrinsic properties of the fuel-air mixture in order to avoid the influence of external parameters, such as the vessel volume or the initial turbulence. To overcome such limitations, the flame propagation of gaseous mixtures is often studied in order to estimate their laminar burning velocity, which is independent of external factors and is a useful input for CFD simulation and for the sizing of protective devices. Experimentally, this parameter is difficult to evaluate when it comes to dust explosion due to the inherent turbulence during the dispersion of the cloud. However, the low inertia of nanoparticles allows performing tests at very low turbulence without sedimentation. Knowledge on flame propagation concerning nanoparticles may then be modelled and, under certain conditions, extrapolated to microparticles, for which an experimental measurement is a delicate task. This work then focused a nanocellulose with primary fiber dimensions of 3 nm width and 70 nm length. A one-dimensional model was developed to estimate the flame velocity of a nanocellulose explosion, based on an existing model already validated for hybrid mixtures of gas and carbonaceous nanopowders similar to soot. Due to the fast devolatilization of organic powders, the chemical reactions considered are limited to the combustion of the pyrolysis gases. The finite volume method was used to solve the mass and energy balances equations and mass reactions rates constituting the numerical system. Finally, the radiative heat transfer was also considered, highlighting the influence of the total surface area of the particles on the thermal radiation. Flame velocities of nanocellulose from 17.5 to 20.8 $cm.s^{-1}$ were obtained numerically depending on the radiative heat transfer, which proves a good agreement with the values around 21 $cm.s^{-1}$ measured experimentally by flame visualization and allows the validation of the model for nanoparticles.

Keywords: *dust explosion, flame propagation, nanoparticles, modeling*

1. Introduction

To mitigate dust explosions, safety barriers such as explosion venting need to be designed by considering the experimental characteristics of the dust explosibility. Such characteristics are routinely determined in a 20 L sphere (Zalosh, 2019) according to well established standards like EN 14034-1 (2004) and EN 14034-2 (2006). This approach only holds by assuming that dust explosibility can be represented by the maximum explosion overpressure value and the Kst. However, such an approach needs to be further questioned as the measurement of dust explosion severity is actually influenced by several parameters such as the initial turbulence (Amyotte et al., 1988; Zhen and Leuckel, 1997), the ignition energy (Zhen and Leuckel, 1997), the moisture content of the powder (Traoré et al., 2009) and the type of nozzle (Dahoe et al., 2001; Murillo et al., 2018; Yao et al., 2020). Beyond these main influential factors, the validity of the so-called ‘cubic law’ (Dahoe et al., 2001) commonly used to extrapolate results obtained in a confined volume to another volume (Eckhoff, 2003) is also questioned.

Standard conditions were initially defined to evaluate the explosion severity of microparticles, but when it comes to nanoparticles, potential discrepancies can arise. Indeed, their small size induces a high specific area and new properties, which can lead to modifications in the combustion kinetics (Bouillard et al., 2010; Dufaud et al., 2011) along with extremely high ignition sensitivity, especially for metallic nanopowders that can spontaneously ignite when exposed to air (Boilard et al., 2013; Krietsch et al., 2015). An evaluation of the adequacy of the current standards for the evaluation of the explosion severity of nanoparticles is then necessary (Santandrea et al., 2019b).

To overcome the identified limitations, direct investigation of the flame propagation could be useful so as to provide fundamental inputs in advanced simulations (CFD or phenomenological approach). The essential parameter is then the laminar burning velocity, which is an intrinsic property of the fuel-air mixture (Belerrajoul, 2019; Dahoe et al., 2002) that can be used in such simulations to evaluate the consequences of an explosion scenario in specific conditions (Skjold, 2003). The existence of a laminar burning velocity of dusts is difficult to define due to the inherent turbulence related to the dispersion of the powder but such an approach was already proposed 30 years ago by Bradley and Lee (1984) though it proved itself challenging when it comes to dusts. Nevertheless, the low inertia and sedimentation rate of nanoparticles enable to investigate flame propagation in very low turbulent conditions (Santandrea et al., 2020).

In this paper, a one-dimensional model initially conceived and validated for hybrid mixtures (Torrado et al., 2018) has been adapted to predict the laminar flame velocity of nanocellulose. Results of simulations are then compared to the experimental values measured on nanocellulose using a flame propagation tube and a vented explosion sphere (Santandrea et al., 2020). The consistency of a correlation established by Silvestrini et al. (2008) to predict laminar flame velocity of micropowders based on the knowledge of their explosion severity was also analyzed for nanocellulose.

2. Material and experimental method

2.1 Flame propagation observation

Nanocellulose powder, or more precisely a cellulose nanocrystals powder NCC (CelluForce), is composed of primary fibers, whose dimensions are 70 nm length and 3 nm width. The flame propagation of nanocellulose was studied at low turbulence by Santandrea et al. (2020) in a flame propagation tube and in a vented visualization 20 L sphere, as summarized in Fig. 1. Due to a difficult visualization of the flame kernel at high concentration, a concentration of 500 $g.m^{-3}$ was chosen, as it is higher than the minimum explosible concentration, i.e. 125 $g.m^{-3}$, to ensure an ignition at low ignition energy, and rather close to the experimental optimal concentration, i.e. 750 $g.m^{-3}$. The particle size distribution of nanocellulose dispersed in both setups was determined using a laser diffraction sensor (Helos - Sympatec). It appears that agglomerates ranging from a few micrometers up to 60 µm are formed in the powder. Explosion were recorded using a high-speed video camera, and the flame kernel growth was analysed in terms of flame front position and surface area using a model developed by Cuervo (2015) in Matlab's Simulink. The equations initially established for gases were then applied to the obtained values, considering that the devolatilization of organic powders is fast and that, under certain concentration and turbulence conditions, the reaction is then limited by the combustion of the pyrolysis gases (Cuervo, 2015; Di Benedetto and Russo, 2007; Dufaud et al., 2012a). Thus, the burning velocity was calculated using the spatial velocity S_u, the estimated cross-section A_s and the flame surface A_f according to Andrews and Bradley (1972), along with the flame stretching factor K, called Karlovitz factor (Karlovitz et al.,1951). Those parameters were then combined to apply a linear relation linking the burning velocity and the Karlovitz factor K to the laminar burning velocity S_{u0} and the Markstein length δ_M, which is a parameter characterizing the stability of the flame (Clavin, 1985; Markstein, 1964).

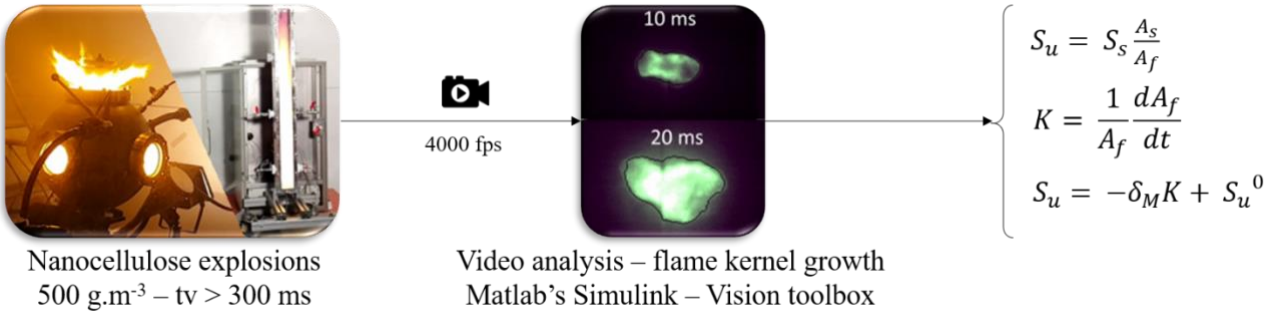

Fig. 1. *Simplified scheme of the experimental determination of the laminar burning velocity by flame visualization used by Santandrea et al. (2020)*

2.2 Pressure-time evolution interpretation

In order to take advantage of the standard explosion tests realized in the 20L sphere, some authors such as Silvestrini et al. (2008) developed a correlation between the laminar burning velocity and the parameters P_{max} and K_{St}. Explosions tests were conducted on nanocellulose in the standard 20 L sphere according to international standards (EN 14034-1, 2004; EN 14034-2, 2006), but using chemical igniters of 100 J to avoid an overdriving phenomenon, knowing the minimum ignition energy of the dried nanocellulose is 5 mJ (Santandrea et al., 2019b). Since the values of laminar burning velocity obtained by flame propagation observation are available only at 500 g.m-3, only the results obtained for this concentration are discussed in this work. Nevertheless, tests were performed over a wide range of dust concentration (up to 1250 g.m-3), and the influence of the dust concentration on the laminar burning velocity is discussed by Santandrea et al. (2020). The laminar burning velocity S_{u0} of starch was then calculated from the knowledge of the explosion overpressure P_m and rate of pressure rise $(dP/dt)_m$, using the correlation established by Silvestrini et al. (2008):

$$S_u{}^0 = 0.11 \frac{\left(\frac{dP}{dt}\right)_m V^{1/3}}{P_m \left(\frac{P_m}{P_0}\right)^{0.14} \left(\frac{P_m}{P_0}\right)^{\left(\frac{1}{\gamma}\right)}} \quad (1)$$

where V is the vessel volume, P_0 the atmospheric pressure and γ the ratio of specific heats. This correlation is based on several assumptions, such as the spherical expansion of the flame, the neglecting of the turbulent length scales and the fact that the burnt gases are trapped behind the expanding flame front (Silvestrini et al., 2008).

3. One-dimensional modelling of flame propagation

Complementary to experiments relying on the flame visualization and the pressure-time evolution, the laminar flame velocity was approached using a one-dimension flame propagation model developed by Torrado et al. (2018) and initially designed to describe gas and hybrid mixtures explosions. The model was then adapted to nanocellulose using the same hypothesis than for flame visualization experiments, i.e. considering a fast devolatilization of the dust and a flame propagation kinetically limited by the combustion of the pyrolysis gases. Moreover, since cellulose and starch are both polymers formed of glucose chains, both compounds are assumed to produce the same pyrolysis gases when tested in the same conditions. Thus, pyrolysis experiments were conducted on wheat starch in a Godbert-Greenwald oven modified according to Dufaud et al. (2012b) to collect the post-pyrolysis gases. The composition obtained for a concentration of approximately 500 g.m-3 and a temperature of 973K was then used as the initial composition of the fuel (Fig. 2) in the model for a numerical determination of the laminar flame velocity of nanocellulose.

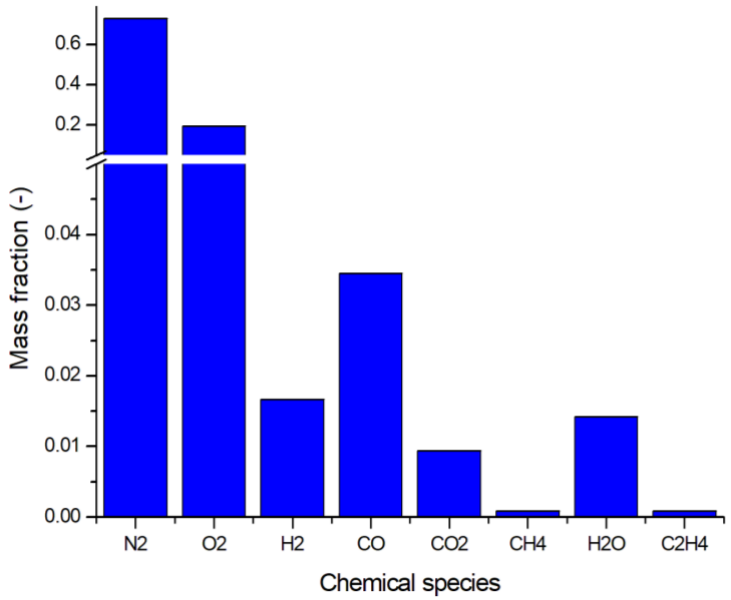

Fig. 2. *Initial composition of the nanocellulose pyrolysis gases/air mixture considered in the flame propagation model for 500 g.m$_3$ of nanocellulose*

The simulation domain is constituted of a horizontal tube with a numerical length of 5 cm involving two parallels walls divided into three distinct zones: preheat, reaction and post-flame, knowing that the flame propagates from the post-flame zone to the preheat zone. Mass, species and energy balances, notably based on the properties of the considered chemical species, were then expressed in the simulation domain. Since the main chemical species constituting the pyrolysis gases of nanocellulose are the same than the species initially considered in the model for the flame propagation of a methane/air flame (Torrado et al., 2018), the same reaction mechanisms were used. However, since the pyrolysis step mainly produced carbon monoxide, a reversible oxidation reaction of this gas to produce carbon dioxide was added (Table 1, reactions 7 and -7).

Table 1: *Reaction mechanisms considered for the combustion of the pyrolysis gases (Units cal, mol, m, s)*

#	Reaction	A_i	β	Ei	Reaction order	Reference
1	$CH_4 + 0.5O_2 \rightarrow CO + 2H_2$	2.45×10^9	0	3×10^4	$[CH_4]^{0.5}\,[O_2]^{1.25}$	(Jones and Lindstedt, 1988)
2	$CH_4 + H_2O \rightarrow CO + 3H_2$	3×10^5	0	3×10^4	$[CH_4]\,[H_2O]$	(Jones and Lindstedt, 1988)
3	$CO + H_2O \rightarrow CO_2 + H_2$	2.75×10^6	0	2×10^4	$[CO]\,[H_2O]$	(Jones and Lindstedt, 1988)
-3	$CO_2 + H_2 \rightarrow CO + H_2O$	9×10^7	0	2.8×10^4	$[CO_2]\,[H_2]$	(Torrado et al., 2018)
4	$H_2 + 0.5O_2 \rightarrow H_2O$	3.85×10^{13}	-1	4×10^4	$[H_2]^{0.25}\,[O_2]^{1.50}$	(Jones and Lindstedt, 1988)
-4	$H_2O \rightarrow H_2 + 0.5O_2$	9.27×10^{18}	0.88	9.8×10^4	$[H_2O]\,[H_2]^{-0.75}\,[O_2]$	(Andersen et al., 2009)
5	$O_2 \rightarrow 2O\cdot$	1.5×10^9	0	1.13×10^5	$[O_2]$	(Frassoldati et al., 2009)
6	$H_2O \rightarrow H\cdot + OH\cdot$	2.3×10^{22}	-3	1.2×10^5	$[H_2O]$	(Frassoldati et al., 2009)

7	$CO + 0.5O_2 \rightarrow CO_2$	1.26×10^4	0	10×10^3	$[CO]\,[O_2]^{0.25}\,[H_2O]^{0.5}$	(Andersen et al., 2009)
-7	$CO_2 \rightarrow CO + 0.5O_2$	1.95×10^{12}	-0.97	78.4×10^3	$[CO_2]\,[H_2O]^{0.5}\,[O_2]^{-0.25}$	(Andersen et al., 2009)

The calculation of the flame velocity then relies on the numerical integration of the differential equations of mass, species and energy. The space derivatives were discretized using the finite volume method with 160 control volumes to obtain a system of ordinary differential equations, which was solved using the integration functions ODE in Matlab. The expression of the mass and species balance, the mass diffusion fluxes and the energy balance, along with the numerical resolution, are properly described by Torrado et al. (2018).

The resolution of the ordinary differential equations requires an initial value of the temperature and mass fractions of all the considered species in every numerical domain. The composition in the preheat zone, which represents 25% of the numerical domain, is defined by the mass fractions of the considered mixture in laboratory conditions. As a first approximation, the mass fractions and temperature are assumed to evolve linearly in the reaction zone, implying those values are known if the initial and final conditions are fixed. To estimate the conditions in the post-flame zone (70% of the considered distance), the adiabatic temperature and mass fraction of the burnt gases for a steady flame were calculated using PREMIX program (Kee et al., 1993). This approach, represented in Fig. 3, was used to reduce the calculation time and to improve the convergence of the program, by initializing all the conditions close to a stable solution. Since this numerical model aims at considering the radiative heat transfer induced by the presence of nanoparticles in the mixture, which is not the case of the PREMIX program, this latter was not considered as a suitable method to determine the laminar burning velocity of nanopowders.

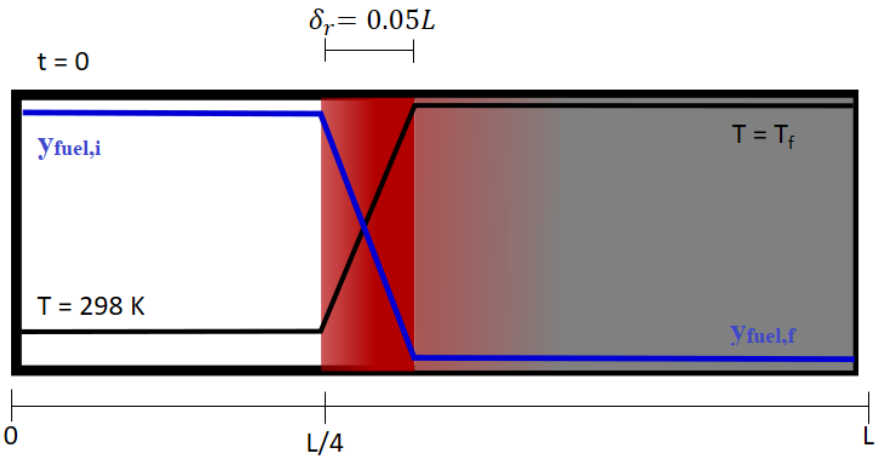

Fig. 3. *Schema of the initial conditions of the temperature and fuel fraction in each zone of the flame (adapted from Torrado et al. (2018))*

The system previously defined was then analyzed considering a distance L of 5 cm and an integration time of 50 ms. The evolution of the temperature with time is presented in Fig. 4 at different positions to describe each zone, knowing that the preheat zone initially spreads up to 1.25 cm and that the post-flame zone starts at 1.5 cm. It appears that, in the post-flame zone (2.5 and 5 cm), the temperature is constant with time, since the reaction already occurred. Then, a fast increase of the temperature after a few milliseconds is visible in the reaction zone, and progressively shifts toward the preheat zone with time, describing the propagation of the flame.

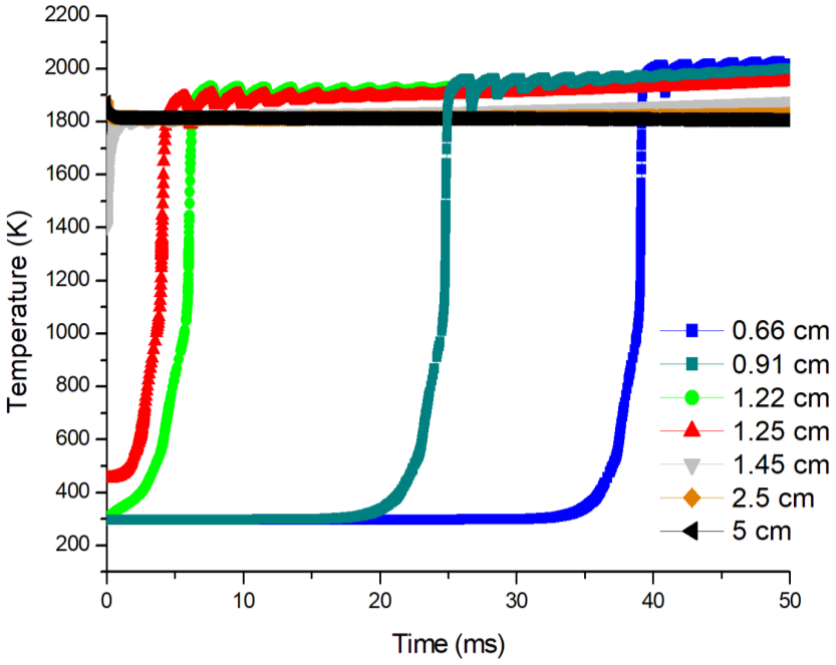

Fig. 4. *Evolution of the temperature with time for different control volumes when modelling the flame propagation of nanocellulose (quiescent conditions, 500 g.m-3)*

4. Results and discussion

4.1 Combustion of the pyrolysis gases

The position of the flame front, assimilated to the position of the highest temperature, was recorded for each integration time and is presented in Fig. ***5***. It should be reminded that the reaction zone was initially located between 1.25 cm and 1.5 cm. However, before 1 ms, a very fast displacement of the flame is observed, preventing a clear determination of the flame front position between 1.4 and 1.5 cm. Nevertheless, a linear evolution of the flame position with time can be observed from 1 ms to 50 ms. A laminar flame velocity of 17.5 cm.s-1, represented by the slope of the linear regression, was then obtained for the combustion of nanocellulose. It should be stressed that this value should be viewed with caution as the pyrolysis step has been considered as very fast with regard to the combustion of the pyrolysis gases, which is a strong assumption.

The flame velocity calculated using the flame propagation model was then compared to the values experimentally obtained by Santandrea et al. (2020) (Table 2). The value determined numerically appears to be of the same order of magnitude than the experimental ones, with a maximum difference of 22% with regard to the laminar flame velocity measured in the flame propagation tube. This value is also consistent with laminar flame velocity of "wood gas" at the stoichiometry mentioned in the literature by Mollenhauer and Tschöke (2010) and Przybyla et al. (2008), reaching around 14 cm.s-1 and 20 cm.s-1 respectively. Nevertheless, this difference between experimental and numerical values can come from experimental uncertainties, but can also be due to the neglecting of the contribution of the radiative heat transfer to the flame propagation. Indeed, if the pyrolysis step can decrease the flame velocity due to a kinetic limitation, the fresh or unburnt remaining particles can also improve the flame propagation through a heat transfer modification in the preheat zone. To evaluate this influence, the contribution of the radiative heat transfer, added to the flame propagation model by Torrado et al. (2018) and based on the work of Haghiri and Bidabadi (2010), is now considered during the combustion of the pyrolysis gases of nanocellulose.

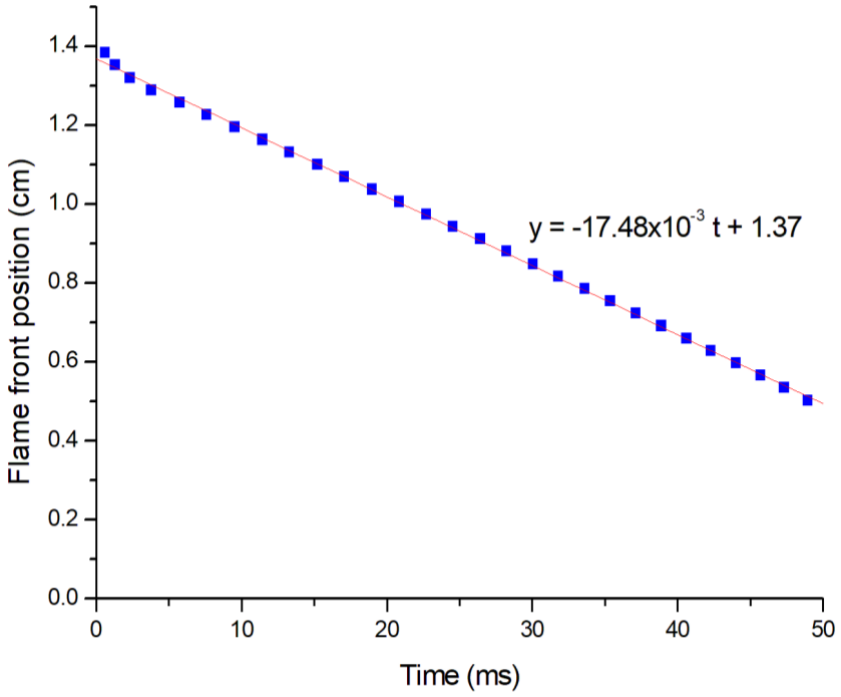

Fig. 5. *Evolution of the flame front position with time during the combustion of nanocellulose pyrolysis gases*

Table 2: *Numerical and experimental values of laminar flame velocity of nanocellulose*

Determination method	**Laminar flame velocity (cm.s^{-1})**
Flame propagation model	17.5
Flame visualization: propagation tube	21.4 ± 1
Flame visualization: vented sphere	20.5 ± 3
Pressure-time evolution: application of Silvestrini et al. (2008) correlation	19.9 ± 3

4.2 Influence of the radiative heat transfer

Since the pyrolysis of nanocellulose particles and the combustion of the pyrolysis gases happen simultaneously, the unburnt particles can impact the flame propagation by variations of the heat transfer. However, the remaining dust can hardly be quantified and characterized for each integration time without taking the pyrolysis kinetics into account. Thus, several dust concentrations, assumed constant with time, were tested. The dust clouds were supposed to be homogeneous over the simulation domain and constituted of monodispersed spherical particles. Moreover, due to the agglomeration of the nanoparticles, the particle size after dispersion must be considered (Santandrea et al., 2019a). Particle size distribution measurements after dispersion of nanocellulose in the 20L sphere led to a mean value of 10 µm (Santandrea et al., 2020). This value was then chosen as a reference for the calculation, along with 100 nm, to represent the primary particles, and 60 µm, which is the mean diameter of nanocellulose agglomerates before dispersion, i.e. the agglomerates not broken by the dispersion process. In this model, Mie scattering, valid for micron particles, was then used to define the radiative heat transfer. It should be noted that Rayleigh scattering, encountered for particles smaller than 100 nm, do not contribute significantly to the flame expansion due to the emission in every direction (Hong and Winter, 2006). Thus, decreasing the particle size below this size would only decrease the radiative heat transfer contributing to the flame propagation, and so the flame velocity. The concentration of dust that did not react during the combustion of the 500 g.m^{-3} of nanocellulose was varied from 2.5 g.m^{-3} to 100 g.m^{-3}, to represent the radiative heat transfer at the

beginning and at the end of the reaction. The radiative heat transfer was then added to the energy balance, and the heat capacity of the dust was then taken into account during the calculation of the mean heat capacity of the mixture. Due to the assumption of a fast pyrolysis, the reactions involving the solid particles were not considered in the model. However, it should be noted that Torrado et al. (2018) evidenced that the contribution of the chemical reactions of the powder is negligible with regard to the contribution of the radiative heat transfer at low concentrations (2.5 g.m^{-3}).

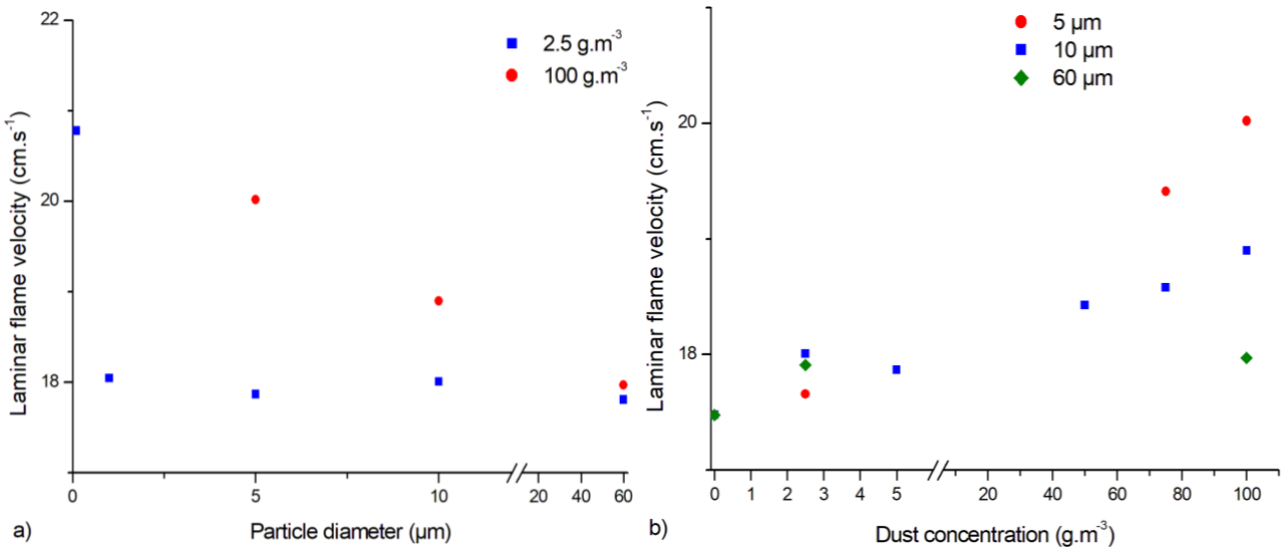

Fig. 6. *Influence of the a) primary diameter and b) of the dust concentration considered for the radiative heat transfer on the laminar flame velocity of nanocellulose (500 g.m^{-3})*

In Figure 6a, it appears that small particles contribute more to the radiative heat transfer than bigger particles in the micro-range. Indeed, particles of 60 µm bring similar contribution to the flame acceleration, i.e. around 0.5 cm.s^{-1}, at 2.5 g.m^{-3} and 100 g.m^{-3}, whereas 100 g.m^{-3} of particles of 5 µm lead to a flame velocity of 20 cm.s^{-1}, i.e. 14% higher than the flame velocity of the pyrolysis gases. It should be underlined that the contribution of particles of 100 nm to the radiative heat transfer may be overestimated since Mie scattering was considered for the calculation whereas Rayleigh scattering is more representative of the heat transfer of nanoparticles. In Figure 6b, it appears that a dust concentration of 2.5 g.m^{-3} leads to a mean flame velocity of around 17.8 cm.s^{-1} for particles between 5 and 60 µm. Increasing the concentration then also increases the contribution of the radiative heat transfer to the flame propagation, reaching 20.0 cm.s^{-1} when considering 100 g.m^{-3} of particles of 5 µm.

Therefore, both the dust concentration and the particle size are of great importance when considering the radiative heat transfer. Indeed, the absorption coefficient K_a and the scattering coefficient K_s directly depend on the dust concentration, the dust density and the particle size, as follows (Haghiri and Bidabadi, 2010):

$$K_a = \frac{3}{2}\frac{C}{\rho_p\, d_p}\, Q_{abs} \tag{2}$$

$$K_s = \frac{3}{2}\frac{C}{\rho_p\, d_p}\, Q_{sca} \tag{3}$$

where C is the dust concentration, ρ_p the particle density, d_p the particle diameter and Q_{abs} and Q_{sca} respectively the absorption and scattering efficiency.

The absorption and scattering coefficients are then directly proportional to the total surface area (TSA) developed by the particles in the cloud, which can be expressed as follows for spherical particles:

$$TSA = \frac{6\,C}{\rho_p\, d_p} \tag{4}$$

A linear evolution of the calculated flame velocity with the total surface area developed by the particles considered in the radiative heat transfer appears in Fig. . Then, it can be observed that the radiative heat transfer generated by particles developing a total surface area lower than 10 $m_2.m_{-3}$ does not lead to a significant increase of the flame velocity, with values between 17.5 and 18 $cm.s_{-1}$. However, when considering a total surface area of 100 $m_2.m_{-3}$, a flame velocity of 20.8 $cm.s_{-1}$ is reached, thus proving the importance of considering the surface area when analysing dust explosions, instead of focusing only on mass concentration. It should also be noted that increasing the concentration too much would lead to an important increase of absorption, which would limit the heat radiation in the preheat zone.

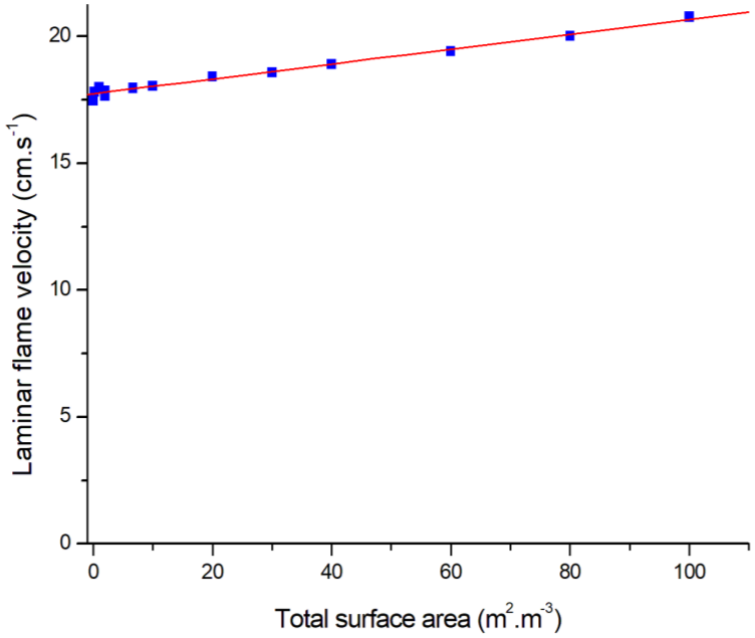

Fig. 7. *Influence of the total surface area of the particles implied in the radiative heat transfer on the flame velocity*

5. Conclusions

The laminar burning velocity of nanocellulose has been determined using a one-dimensional flame propagation model adapted from a model already validated for hybrid mixtures. The numerical system, composed of mass and energy balances equations and of mass reaction rates adapted to the combustion reactions, was solved by the finite volume method. Since the devolatilization of organic powders is fast, the chemical reactions were considered limited to the combustion of the pyrolysis gases. A first value of laminar flame velocity of 17.5 $cm.s_{-1}$ was obtained for 500 $g.m_{-3}$ of nanocellulose, which is close to values experimentally measured in a flame propagation tube or a 20 L sphere, around 21 $cm.s_{-1}$, thus showing a good consistency between the numerical and experimental approaches.

However, since, in practice, the devolatilization of the particles is not instantaneous, the remaining particles can contribute to the radiative heat transfer, which was added to energy balance. Due to the tendency of nanoparticles to agglomerate, different particle diameters and dust concentrations were tested. Thus, although the heat transfer of nanoparticles tends to be neglected due to Rayleigh scattering, which does not contribute to the flame propagation, the contribution of the remaining micro-agglomerates after dispersion must be considered. Indeed, the existence of a linear relation

between the laminar flame velocity and the total surface area developed by the particles implied in the radiative heat transfer was highlighted. A flame velocity reaching 20.8 $cm.s^{-1}$ for a total surface area of 100 $m^2.m^{-3}$ considered for the radiative heat transfer was then obtained, showing a strong impact of the heat radiation on the flame propagation.

Acknowledgements

This work was supported financially by the French Ministry for the Ecological and Solidary Transition and The French Ministry for Higher Education and Research.

References

Amyotte, P.R., Chippett, S., Pegg, M.J., 1988. Effects of turbulence on dust explosions. Progress in Energy and Combustion Science 14, 293–310. https://doi.org/10.1016/0360-1285(88)90016-0

Andersen, J., Rasmussen, C.L., Giselsson, T., Glarborg, P., 2009. Global Combustion Mechanisms for Use in CFD Modeling under Oxy-Fuel Conditions. Energy & Fuels 23, 1379–1389. https://doi.org/10.1021/ef8003619

Andrews, G.E., Bradley, D., 1972. Determination of burning velocities: A critical review. Combustion and Flame 18, 133–153. https://doi.org/10.1016/S0010-2180(72)80234-7

Belerrajoul, M., 2019. Modélisation multi-échelle de la combustion d'un nuage de particules (PhD Thesis). National Polytechnic Institute of Toulouse.

Boilard, S.P., Amyotte, P.R., Khan, F.I., Dastidar, A.G., Eckhoff, R.K., 2013. Explosibility of micron- and nano-size titanium powders. Journal of Loss Prevention in the Process Industries 26, 1646–1654. https://doi.org/10.1016/j.jlp.2013.06.003

Bouillard, J., Vignes, A., Dufaud, O., Perrin, L., Thomas, D., 2010. Ignition and explosion risks of nanopowders. Journal of Hazardous Materials 181, 873–880. https://doi.org/10.1016/j.jhazmat.2010.05.094

Bradley, D., Lee, J.H.S., 1984. . Proceedings of the first international colloquium on the explosibility of industrial dusts 220–223.

Clavin, P., 1985. Dynamic behavior of premixed flame fronts in laminar and turbulent flows. Progress in Energy and Combustion Science 11, 1–59. https://doi.org/10.1016/0360-1285(85)90012-7

Cuervo, N., 2015. Influences of turbulence and combustion regimes on explosions of gas-dust hydrid mixtures (PhD Thesis). The University of Lorraine, France.

Dahoe, A.E., Cant, R.S., Scarlett, B., 2001. On the Decay of Turbulence in the 20-Liter Explosion Sphere. Flow, Turbulence and Combustion 67, 159–184. https://doi.org/10.1023/A:1015099110942

Dahoe, A.E., Hanjalic, K., Scarlett, B., 2002. Determination of the laminar burning velocity and the Markstein length of powder–air flames. Powder Technology, Special issue i in Honour of Prof Jimbo 122, 222–238. https://doi.org/10.1016/S0032-5910(01)00419-3

Di Benedetto, A., Russo, P., 2007. Thermo-kinetic modelling of dust explosions. Journal of Loss Prevention in the Process Industries, Selected Papers Presented at the Sixth International Symposium on Hazards, Prevention and Mitigation of Industrial Explosions 20, 303–309. https://doi.org/10.1016/j.jlp.2007.04.001

Dufaud, O., Khalili, I., Cuervo-Rodriguez, N., Olcese, R.N., Dufour, A., Perrin, L., Laurent, A., 2012a. Highlighting the Importance of the Pyrolysis Step on Dusts Explosions. Chemical Engineering Transactions 26, 369–374.

Dufaud, O., Poupeau, M., Khalili, I., Cuervo, N., Christodoulou, M., Olcese, R., Dufour, A., Perrin, L., 2012b. Comparing Pyrolysis Gases and Dusts Explosivities: A Clue to Understanding Hybrid Mixtures Explosions? Ind. Eng. Chem. Res. 51, 7656–7662. https://doi.org/10.1021/ie201646s

Dufaud, O., Vignes, A., Henry, F., Perrin, L., Bouillard, J., 2011. Ignition and explosion of nanopowders: something new under the dust. Journal of Physics: Conference Series 304, 012076. https://doi.org/10.1088/1742-6596/304/1/012076

Eckhoff, R.K., 2003. Dust Explosions in the Process Industries - 3rd Edition, 3rd ed. Gulf Professional Publishing.

EN 14034-1, 2004. Determination of explosion characteristics of dust clouds — Part 1: Determination of the maximum explosion pressure □max of dust clouds.

EN 14034-2, 2006. Determination of explosion characteristics of dust clouds — Part 2: Determination of the maximum rate of explosion pressure rise (dp/dt)max of dust clouds.

Frassoldati, A., Cuoci, A., Faravelli, T., Ranzi, E., Candusso, C., Tolazzi, D., 2009. Simplified kinetic schemes for oxy-fuel combustion. 1 st International Conference on Sustainable Fossil Fuels for Future Energy – S4FE 2009.

Haghiri, A., Bidabadi, M., 2010. Modeling of laminar flame propagation through organic dust cloud with thermal radiation effect. International Journal of Thermal Sciences 49, 1446–1456. https://doi.org/10.1016/j.ijthermalsci.2010.03.013

Hong, S.-H., Winter, J., 2006. Size dependence of optical properties and internal structure of plasma grown carbonaceous nanoparticles studied by *in situ* Rayleigh-Mie scattering ellipsometry. Journal of Applied Physics 100, 064303. https://doi.org/10.1063/1.2338132

Jones, W.P., Lindstedt, R.P., 1988. Global reaction schemes for hydrocarbon combustion. Combustion and Flame 73, 233–249. https://doi.org/10.1016/0010-2180(88)90021-1

Karlovitz, B., Denniston, D.W., Wells, F.E., 1951. Investigation of Turbulent Flames. J. Chem. Phys. 19, 541–547. https://doi.org/10.1063/1.1748289

Kee, R.J., Grcar, J.F., Smooke, M.D., Miller, J.A., Meeks, E., 1993. PREMIX: A FORTRAN Program for Modeling Steady Laminar One-Dimensional Premixed Flames.

Krietsch, A., Scheid, M., Schmidt, M., Krause, U., 2015. Explosion behaviour of metallic nano powders. Journal of Loss Prevention in the Process Industries 36, 237–243. https://doi.org/10.1016/j.jlp.2015.03.016

Markstein, G.H., 1964. Non-steady flame Propagation. P22, Pergarmon, New York.

Mollenhauer, K., Tschöke, H., 2010. Handbook of Diesel Engines. Springer Science & Business Media.

Murillo, C., Amín, M., Bardin-Monnier, N., Muñoz, F., Pinilla, A., Ratkovich, N., Torrado, D., Vizcaya, D., Dufaud, O., 2018. Proposal of a new injection nozzle to improve the experimental reproducibility of dust explosion tests. Powder Technology 328, 54–74. https://doi.org/10.1016/j.powtec.2017.12.096

Przybyla, G., Ziolkowski, L., Szlęk, A., 2008. Performance of SI engine fuelled with LCV gas. Poland: Institute of Thermal Technology.

Santandrea, A., Gavard, M., Pacault, S., Vignes, A., Perrin, L., Dufaud, O., 2020. 'Knock on nanocellulose': Approaching the laminar burning velocity of powder-air flames. Process Safety and Environmental Protection 134, 247–259. https://doi.org/10.1016/j.psep.2019.12.018

Santandrea, A., Pacault, S., Perrin, L., Vignes, A., Dufaud, O., 2019a. Nanopowders explosion: Influence of the dispersion characteristics. Journal of Loss Prevention in the Process Industries 62, 103942. https://doi.org/10.1016/j.jlp.2019.103942

Santandrea, A., Vignes, A., Krietsch, A., Perrin, L., Laurent, A., Dufaud, O., 2019b. Some Key Considerations when Evaluating Explosion Severity of Nanopowders. Chemical Engineering Transactions 77, 235–240. https://doi.org/10.3303/CET1977040

Silvestrini, M., Genova, B., Leon Trujillo, F.J., 2008. Correlations for flame speed and explosion overpressure of dust clouds inside industrial enclosures. Journal of Loss Prevention in the Process Industries 21, 374–392. https://doi.org/10.1016/j.jlp.2008.01.004

Skjold, T., 2003. Selected aspects of turbulence and combustion in 20-Litre explosion vessel (Master thesis). University of Bergen, Norway.

Torrado, D., Pinilla, A., Amin, M., Murillo, C., Munoz, F., Glaude, P.-A., Dufaud, O., 2018. Numerical study of the influence of particle reaction and radiative heat transfer on the flame velocity of gas/nanoparticles hybrid mixtures. Process Safety and Environmental Protection 118, 211–226. https://doi.org/10.1016/j.psep.2018.06.042

Traoré, M., Dufaud, O., Perrin, L., Chazelet, S., Thomas, D., 2009. Dust explosions: How should the influence of humidity be taken into account? Process Safety and Environmental Protection, 12th International Symposium of Loss Prevention and Safety Promotion in the Process Industries 87, 14–20. https://doi.org/10.1016/j.psep.2008.08.001

Yao, N., Wang, L., Bai, C., Liu, N., Zhang, B., 2020. Analysis of dispersion behavior of aluminum powder in a 20 L chamber with two symmetric nozzles. Process Safety Progress 39. https://doi.org/10.1002/prs.12097

Zalosh, R., 2019. Dust explosions: Regulations, standards, and guidelines, in: Methods in Chemical Process Safety. Elsevier, pp. 229–282. https://doi.org/10.1016/bs.mcps.2019.03.003

Zhen, G., Leuckel, W., 1997. Effects of ignitors and turbulence on dust explosions. Journal of Loss Prevention in the Process Industries 10, 317–324. https://doi.org/10.1016/S0950-4230(97)00021-1